

Controlling Avatar Diffusion with Learnable Gaussian Embedding

Xuan Gao Jingtao Zhou Dongyu Liu Yuqi Zhou Juyong Zhang*

University of Science and Technology of China



Figure 1. We introduce a novel diffusion control signal representation splatted from learnable Gaussians, which is dense, adaptive, expressive, and 3D-consistent. Additionally, we incorporate a real/synthetic token to minimize artifact contamination of the synthetic dataset. Given a single reference image, our model can achieve high-quality, expressive, and consistent head generation.

Abstract

Recent advances in diffusion models have made significant progress in digital human generation. However, most existing models still struggle to maintain 3D consistency, temporal coherence, and motion accuracy. A key reason for these shortcomings is the limited representation ability of commonly used control signals (e.g., landmarks, depth maps, etc.). In addition, the lack of diversity in identity and pose variations in public datasets further hinders progress in this area. In this paper, we analyze the shortcomings of current control signals and introduce a novel control signal representation that is optimizable, dense, expressive, and 3D consistent. Our method embeds a learnable neural Gaussian onto a parametric head surface, which greatly enhances the consistency and expressiveness of diffusion-based head models. Regarding the dataset, we synthesize a large-scale dataset with multiple poses and identities. In addition, we use real/synthetic labels to effectively distinguish real and synthetic data, minimizing the impact of imperfections in synthetic data on the generated head images. Extensive experiments show that our model out-

performs existing methods in terms of realism, expressiveness, and 3D consistency. Our code, synthetic datasets, and pre-trained models will be released in our project page: <https://ustc3dv.github.io/Learn2Control/>

1. Introduction

Generalizable head modeling has wide applications in AR/VR, film, and entertainment industries. Ensuring high-fidelity rendering while maintaining 3D consistency, temporal consistency, and identity generalization still remains a major challenge. Constructing a powerful head model depends heavily on how the head is represented, how the generative model is trained, and high-quality training datasets.

Early generalizable head models [1, 5, 38, 61] generally use meshes to represent the head, but this representation method faces many challenges, such as difficulty in modeling non-facial areas, and unrealistic rendering effects. Some methods use implicit functions [13, 14, 28, 40, 58, 62, 63, 102] or 3D Gaussians [9, 78] to model the head, further improving the rendering effect of the model. Although these methods have achieved some success, they mainly adopt a one-to-one mapping paradigm, while the relationship be-

*Corresponding Author

tween the control signal and the rendered head image is essentially one-to-many. The one-to-one design seriously hinders the expressiveness and generalization ability of the model.

Diffusion models have demonstrated remarkable capabilities in addressing one-to-many problems. Most recent works employ landmarks, normal maps, or depth maps as signals to control the generation of digital humans. Despite some successes achieved by these approaches, we observe that their results still suffer from deficiencies in 3D consistency and expression accuracy. These deficiencies in the generation results are closely related to the control signals used by these diffusion models. For example, the information of landmarks is too sparse, making it hard to capture detailed facial muscle movements or accurately describe head poses. Depth maps and normal maps only represent specific geometric attributes and are inherently camera-dependent, lacking 3D consistency. When such 3D inconsistent control signals are introduced into diffusion, the inconsistency in the generation results is further amplified.

In addition to the representation of control signals, improving data quality and diversity is also crucial for the ability of the trained model. Some studies have utilized game engines to generate synthetic data [3, 68, 91] to meet the requirements of extensive training data. However, due to the inherent authenticity gap between synthetic data and real data, models trained on these data usually often struggle to produce highly realistic results, or need to be fine-tuned for specific subject to improve the results.

As shown in Figure 1, in this paper, we introduce a powerful and generalizable diffusion avatar, which is empowered by a learnable Gaussian embedding control signal and a diverse synthetic human head dataset. Different from all existing control signals for digital head generation, we no longer rely on visual cues like landmarks, normal maps, or depth maps, but instead embed a learnable Gaussian field onto the parameterized head surface [37]. This allows the model to adaptively learn and interpret local geometric features. Compared to landmarks, this representation provides a denser spatial representation, and compared to normal or depth maps, it is 3D consistent and conveys richer semantic information. The splatted Gaussian feature map is then injected into a reference-based denoising framework to generate high-quality avatars.

To enhance the model’s robustness under different viewpoints, we further introduce a synthetic dataset. Unlike previous methods that rely on game engines for data synthesis, we leverage a state-of-the-art 3D head generative model [36] to generate data that closely aligns with the distribution of real human heads. This results in a high-quality dataset with rich identity diversity and a large number of pose variations. In addition, we incorporate a learnable token into the cross-attention module of U-Net, enabling the model to dis-

tinguish between generated and synthetic data. This helps prevent artifacts of synthetic data from affecting the realism of the generated results.

In summary, our contributions include the following aspects:

- We propose a new digital head control signal. Instead of relying on existing visual cues, we leverage feature maps with learnable Gaussian embeddings, significantly enhancing the consistency and authenticity of the generated results.
- To address the limitations of existing public datasets in terms of identity diversity and pose richness, we propose to use synthetic data to improve the ability of the trained model, and use real/synthetic labels to eliminate the impact of artifacts in synthetic data on generated results.
- Experiments show that our model is significantly better than previous works in terms of expressiveness and consistency. It should be noted that the proposed control signal representation and training data synthesis and utilization mechanism is also expected to be extended to more general 3D digital content generation.

2. Related Work

2.1. Generalizable Head Avatars

Mesh-based head models have been extensively studied over the years. Some approaches [32, 53, 77] incorporate neural rendering techniques to enhance face rendering quality. However, due to the inherent limitations of mesh representations, it is still hard to capture detailed facial motions and model non-facial regions. Recent advancements have leveraged NeRF [47] to achieve photo-realistic head rendering. Some methods integrate parametric facial priors with MLPs [3, 28, 102], tri-planes [10, 39, 41, 44, 58, 71, 84, 87], manifolds [72] or volumetric primitives [6] to enhance controllability and disentanglement within radiance fields. Others learn the disentanglement under the help of some pre-trained motion model [13] or directly from data [14, 62, 63]. Some recent works utilize 3D Gaussians [31] as primitives to model generalizable head avatars [9, 78]. Another line of works [19, 85, 97] mainly focus on detailed head geometry. Instead of using radiance field, they use SDF value to accurately represent the surface.

2.2. Non-diffusion-based Head Animation

Face animation has been studied for a long time. Some methods [22, 26, 27, 45, 56, 57, 69, 95] have utilized implicit keypoints as an intermediate motion representation to warp the source portrait. By encoding expressions as latent vectors and injecting them into generator networks, some methods [4, 15, 16, 65, 89, 98] seek to map driving facial movements onto synthesized portraits via feature-space manipulation. Although these methods have achieved

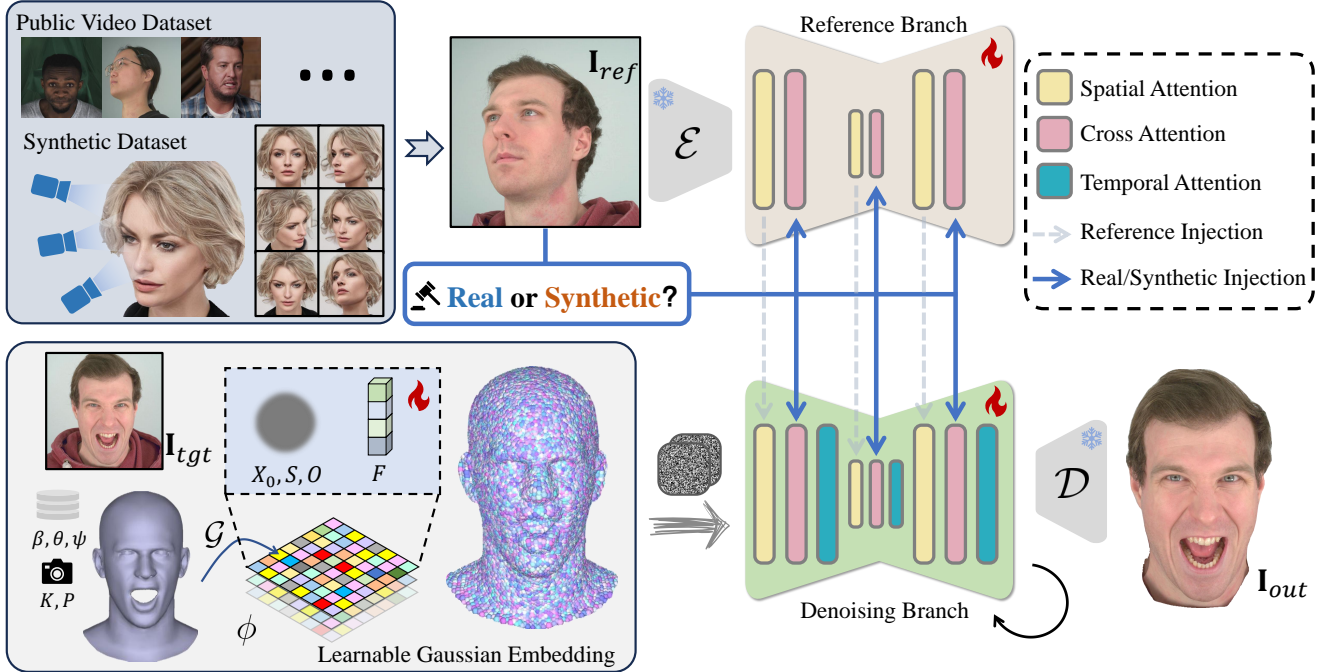


Figure 2. Our pipeline. To address the limitations of existing public datasets in terms of identity diversity and pose richness, we propose to use synthetic data to improve the generalization ability and view consistency of the trained model. We first track the FLAME coefficients of the driving frames \mathcal{I}_{tgt} . Then the learnable Gaussians in UV space are transformed to 3D space according to FLAME UV mapping. Subsequently, the transformed Gaussians are projected and splatted to serve as control signals for a reference-guided diffusion model.

some success, due to the lack of human head priors, they may exhibit some artifacts, particularly under extreme pose changes or large expression variations. Some animation models [18, 52, 60, 86, 94] integrate 3DMM priors [1] into GANs, but their 3D consistency and rendering quality are not satisfying enough.

2.3. Diffusion-based Head Generation

Denoising Diffusion Models [25] have demonstrated remarkable generative capabilities in computer vision. Early works primarily leveraged diffusion models for single-image generation [23, 50, 67] or editing [2, 96]. FADM [90] was the first diffusion based portrait animation model. More recent works have integrated shared attention mechanisms to inject reference information into the denoising network. Some approaches employ synthetic cross-identity data pairs to enable direct animation driven by real images [76, 83], while others utilize landmarks, normal maps, or depth maps as control signals [43, 51, 70, 82]. Additionally, multi-modal control signal integration [21, 79, 99, 101] and attention-based region enhancement [82] have been explored to improve animation realism and flexibility. There also exist some works that construct the diffusion process in UV space [35] or tri-plane space [68, 91]. The most closely related works to this paper are DiffusionAvatars [34], ConsistentAvatar [81] and Stable Video Portraits [48]. While all

have demonstrated some success in diffusion-based avatar rendering, they require subject-specific training.

Another research direction focuses on leveraging 2D diffusion priors for 3D portrait construction. Some methods utilize multi-view diffusion models to ensure view consistency in generated portraits [8, 20, 24, 30, 42, 46, 59]. Others distill image diffusion priors into the construction process [17, 92] for high quality portrait generation.

3. Method

Given a reference image $\mathbf{I}_{ref} \in \mathbb{R}^{H \times W \times 3}$ and a target sequence with length N , denoted as $\mathcal{I}_{tgt} = \{\mathbf{I}_{tgt}^n \in \mathbb{R}^{H \times W \times 3} | n \in [1, N]\}$. Our goal is to generate a corresponding output sequence $\mathcal{I}_{out} = \{\mathbf{I}_{out}^n \in \mathbb{R}^{H \times W \times 3} | n \in [1, N]\}$. The generated sequence should faithfully follow the motion in \mathcal{I}_{tgt} while preserving the identity in \mathbf{I}_{ref} . The overall pipeline of our approach is illustrated in Figure 2. We begin with an overview of Stable Diffusion [54] in Section 3.1, which serves as the backbone of our approach. In Section 3.2, we introduce a novel learnable control signal empowered by learnable Gaussian embedding. Next, in Section 3.3, we inject the splatted head features into a reference-guided diffusion model, ensuring that the generated motion aligns with \mathcal{I}_{tgt} while maintaining identity consistency with \mathbf{I}_{ref} . To further unleash the potential of our model, in Section 3.4, we generate a synthetic multi-view

dataset to enhance the identity diversity and view consistency of our model.

3.1. Preliminary: Stable Diffusion

Stable Diffusion (SD) [54] performs the diffusion process in the latent space rather than directly on pixel space. Given an input image $\mathbf{I} \in \mathbb{R}^{H \times W \times 3}$, the encoder \mathcal{E} maps it into a lower-dimensional latent representation: $\mathbf{z} = \mathcal{E}(\mathbf{I}) \in \mathbb{R}^{h \times w \times \text{channel}}$. The decoder \mathcal{D} then reconstructs the image from this latent space: $\mathbf{I}_{recon} = \mathcal{D}(\mathbf{z})$.

SD learns to denoise an unstructured Gaussian noise ϵ to \mathbf{z} in real image latent domain according to some given condition c . During training, the image latent \mathbf{z} is diffused in t timesteps to produce noise latent \mathbf{z}_t . A denoising U-Net is trained to recover the original structure of \mathbf{z}_t . At inference, \mathbf{z}_T is initially sampled from a standard Gaussian distribution at timestep T and is progressively denoised and restored to \mathbf{z}_0 . A typical block in its U-Net includes three types of computations: 2D convolution, self-attention [64], and cross-attention. Cross-attention is conducted between condition c and block features.

3.2. Learnable Gaussian Embedding

3.2.1. Gaussian Representation

We leverage 3D Gaussians [31] as geometric primitives to represent the head scene. These Gaussian primitives provide an adaptive and flexible representation of geometry, enabling more expressive control over head motion. The Gaussian primitive is defined by a 3D covariance matrix Σ centered at a point \mathbf{x}_0 :

$$g(\mathbf{x}) = e^{-\frac{1}{2}(\mathbf{x}-\mathbf{x}_0)^T \Sigma^{-1}(\mathbf{x}-\mathbf{x}_0)}. \quad (1)$$

The covariance matrix Σ can be decomposed into a rotation matrix R and a scaling matrix Λ :

$$\Sigma = R \Lambda \Lambda^T R^T. \quad (2)$$

We empirically found that using isotropic Gaussians as diffusion control signals yielded results similar to those obtained with anisotropic Gaussians. Therefore, we simplify the representation by setting $\Lambda = sI$. Since $RR^T = I$, the original quaternion \mathbf{q} is no longer needed, leading to a simplified Gaussian formulation:

$$g(\mathbf{x}) = e^{-\frac{1}{2s} \|\mathbf{x}-\mathbf{x}_0\|_2^2}. \quad (3)$$

Each 3D Gaussian is additionally assigned two attributes: opacity o and a learnable feature \mathbf{f} . The final simplified Gaussian can be written as $\{\mathbf{x}_0, s, o, \mathbf{f}\}$, while the entire Gaussian field is written as (X_0, S, O, F) .

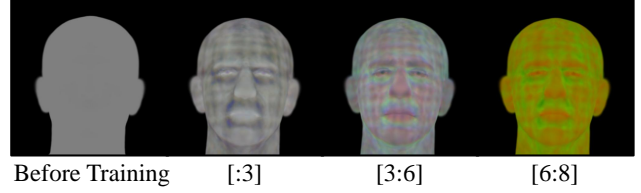


Figure 3. Visualization of the 8 channels of \mathbf{F} . Before training, the feature maps exhibited no meaningful facial information. After training, they developed into highly expressive representations.

3.2.2. Surface-embedded Gaussian Field

We first track \mathcal{I}_{tgt} to get parameters $\mathcal{X} = \{(\beta, \theta_n, \psi_n, K_n, P_n) | n \in [1, N]\}$. Here β, θ_n, ψ_n represent FLAME [37] shape, pose, and expression coefficients, while K, P correspond to the camera’s intrinsic and extrinsic parameters.

Similar to FlashAvatar [74], we maintain a 3D Gaussian field on the UV space of the FLAME model [37], and further deform the Gaussians according to the deformation of underlying meshes. To be specific, we have a learnable Gaussian field ϕ in the FLAME UV domain where each pixel is characterized by three attributes: learnable feature \mathbf{f} , opacity o , scale s . Using UV mapping $\mathcal{G} \in \mathbb{R}^3 \rightarrow \mathbb{R}^2$, we transform the learnable Gaussians from UV space to 3D space. This operation \mathcal{H} could be written as:

$$(X_0, S, O, F) = \mathcal{H}(M(\beta, \theta, \psi), \mathcal{G}, \phi), \quad (4)$$

where $M(\beta, \theta, \psi)$ is the FLAME surface. Given $M(\beta, \theta, \psi)$, \mathcal{G} and ϕ , we could get the 3D Gaussians (X_0, S, O, F) corresponding to a certain frame. Then given camera’s intrinsics K and extrinsics P , the splatted 2D feature map is computed by sorting and blending overlapped 3D Gaussians following [31]:

$$\mathbf{F} = \sum_m \mathbf{f}_m \alpha_m \prod_{j=1}^{m-1} (1 - \alpha_j), \quad (5)$$

where α_m is obtained by multiplying the projected Gaussian with its opacity o .

\mathbf{F} is then used as control signal for the diffusion model in Section 3.3. Compared with previous works that utilize visual cues like landmarks, normal maps, or depth maps as head control signals, our proposed control signals are:

- **Dense** Unlike sparse landmark-based representations, the splatted feature map \mathbf{F} provides a dense encoding of head shape and motion. This allows it to capture fine-grained deformations of the FLAME surface, such as subtle facial muscle movements.
- **Adaptive** The joint optimization of learnable Gaussians and the denoising network enables the model to autonomously learn how to interpret local geometric features, significantly enhancing control accuracy.

- **Expressive** Instead of storing colors or SH coefficients as Gaussian attributes, using a neural feature \mathbf{f} make it possible to map the surface $M(\beta, \theta, \psi)$ into a high-dimensional feature space, the overlapped Gaussians may exhibit more complex and expressive patterns.
- **3D Consistent** It is worth noting that both normal maps and depth maps are not inherently 3D consistent, as their pixel values vary based on camera parameters. This further increases the learning burden of the denoising network and causes the inconsistency in final generated results. In contrast, our neural Gaussian head prior is a view-independent representation, which naturally encourage 3D consistency in the generated results.
- **Easy for Cross-identity Reenactment** The FLAME model inherently possesses disentangled identity and expression spaces. For a cross-identity driving task, one only needs to replace the shape coefficients β with the shape coefficients of reference image β_{ref} to replace identity in control signals.

3.3. Reference-Guided Denoising

With the learnable control signals proposed in Section 3.2, the parameter sequence \mathcal{X} can be transformed into a feature map sequence $\mathcal{C} = \{\mathbf{F}_n | n \in [1, N]\}$. In this subsection, we utilize a reference-guided denoising framework to learn the relationship between \mathcal{C} and \mathcal{I}_{tgt} . Our framework contains a dual-branch paradigm including a reference branch and a denoising branch.

3.3.1. Reference Branch

Recent works have demonstrated that using a ReferenceNet [7, 29, 80] can significantly improve detail preservation, thanks to its multi-scale shared attention injection mechanism. In our implementation, ReferenceNet follows the same architecture as Stable Diffusion. Given the reference image \mathbf{I}_{ref} , we first encode the reference image with \mathcal{E} . Then \mathbf{z}_{ref} is passed through ReferenceNet. The feature maps in each transformer block of ReferenceNet are injected into the corresponding blocks of the denoising branch via shared attention.

3.3.2. Denoising Branch

Given the noised latent \mathbf{z}_t and feature map sequence \mathcal{C} , the denoising network is trained to reconstruct the original structure of \mathbf{z}_t . We downsample \mathcal{C} with the pose guidance network in [99] and add the feature to U-Net encoder. Every transformer block in denoising U-Net performs shared attention to integrate reference branch features into the denoising computation in a block-wise manner. Following previous video generation works [7, 29, 80], temporal layers are applied to each block of the denoising U-Net to guarantee temporal consistency.

| | ID | Views | In the wild |
|-----------------------|--------------|--------------|---------------|
| D3DFACS [11] | 10 | 6 | NO |
| NerSemble [33] | 268 | 16 | NO |
| i3DMM [85] | 64 | 137 | NO |
| HUMBI [88] | 772 | 68 | NO |
| Multiface [73] | 13 | 160 | NO |
| RenderMe [49] | 500 | 60 | NO |
| FaceScape [100] | 847 | 68 | NO (with cap) |
| MEAD [66] | 48 | 7 | NO |
| Our Synthetic Dataset | 10000 | Dense | YES |

Table 1. Comparison with existing multi-view head datasets

3.3.3. Loss function

We use v-parameterization [55] and the only loss function is:

$$\mathcal{L}(\theta, \phi) = \mathbb{E}_{\mathbf{z}_0, t, \epsilon} (\|v_\theta(\mathbf{z}_t, \mathcal{C}, \mathbf{z}_{ref}) - v\|_2^2) \quad (6)$$

As illustrated in Figure 3, there is no need to directly supervise \mathbf{F}_n . Instead, the Gaussian features \mathbf{f} naturally develop into highly expressive representations under the guidance of the denoising loss function, highlighting the inherently adaptive nature of our control signal representation.

3.4. Synthetic Head Dataset

Previous works primarily rely on talking head datasets for training, but most talking head videos contain limited pose or expression variations. As a result, models trained on these datasets lack robustness to large poses. Recent works have attempted to improve this by training the diffusion models using multi-view datasets or some internal large-pose datasets. However, the number of subjects in these datasets is often limited (typically fewer than 1000), which is insufficient to train a model with strong identity generalization. In this work, we employ SphereHead [36] to generate a large-scale dataset with diverse poses and identities, significantly enhancing the pose robustness and identity generalization of reference-guided diffusion models.

3.4.1. Dataset Generation

Given a random noise input, SphereHead renders 3D-consistent head images of a certain subject. For each subject, we randomly sample with yaw angles in $[-60^\circ, 60^\circ]$ and pitch angles in $[-30^\circ, 45^\circ]$, rendering approximately 60 images per subject. In total, we synthesize 10,000 unique subjects. We then fit FLAME models [37] to each subject’s multi-view images to estimate camera poses and FLAME coefficients.

3.4.2. Mitigating Contamination

Although synthetic images provide rich identity diversity, they often exhibit artifacts, particularly in regions such as ears, teeth, and eyeglasses. To prevent these artifacts from

| Method | Self Reenactment | | | | | | | Cross Reenactment | | |
|------------------------|------------------|-----------------|--------------------|-----------------|-----------------|------------------|------------------|-------------------|------------------|------------------|
| | PSNR \uparrow | SSIM \uparrow | LPIPS \downarrow | L1 \downarrow | CSIM \uparrow | AED \downarrow | APD \downarrow | CSIM \uparrow | AED \downarrow | APD \downarrow |
| ROME [32] | 25.77 | 0.878 | 0.132 | 0.022 | 0.610 | 0.155 | 0.016 | 0.426 | 0.242 | 0.025 |
| Portrait4D-v2 [14] | 27.39 | 0.887 | 0.104 | 0.018 | 0.792 | 0.135 | 0.022 | 0.584 | 0.247 | 0.028 |
| VOODOO 3D [63] | 22.10 | 0.856 | 0.152 | 0.034 | 0.499 | 0.171 | 0.045 | 0.357 | 0.250 | 0.054 |
| GAGAvatar [9] | 26.58 | 0.886 | 0.117 | 0.019 | 0.810 | 0.143 | 0.030 | 0.599 | 0.247 | 0.037 |
| Follow-Your-Emoji [43] | 26.39 | 0.878 | 0.111 | 0.019 | 0.792 | 0.176 | 0.023 | 0.432 | 0.388 | 0.118 |
| X-Portrait [76] | 26.47 | 0.878 | 0.103 | 0.020 | 0.813 | 0.137 | 0.019 | 0.416 | 0.335 | 0.152 |
| Ours | 27.84 | 0.890 | 0.099 | 0.016 | 0.831 | 0.123 | 0.014 | 0.648 | 0.232 | 0.023 |

Table 2. Quantitative results on the VFHQ [75] testset.

| Method | Self Reenactment | | | | | | | Cross Reenactment | | |
|------------------------|------------------|-----------------|--------------------|-----------------|-----------------|------------------|------------------|-------------------|------------------|------------------|
| | PSNR \uparrow | SSIM \uparrow | LPIPS \downarrow | L1 \downarrow | CSIM \uparrow | AED \downarrow | APD \downarrow | CSIM \uparrow | AED \downarrow | APD \downarrow |
| ROME [32] | 24.06 | 0.892 | 0.155 | 0.030 | 0.331 | 0.216 | 0.025 | 0.424 | 0.262 | 0.030 |
| Portrait4D-v2 [14] | 25.56 | 0.892 | 0.134 | 0.024 | 0.495 | 0.224 | 0.030 | 0.589 | 0.271 | 0.035 |
| VOODOO 3D [63] | 22.38 | 0.878 | 0.152 | 0.036 | 0.317 | 0.231 | 0.040 | 0.349 | 0.295 | 0.047 |
| GAGAvatar [9] | 25.19 | 0.902 | 0.144 | 0.025 | 0.450 | 0.231 | 0.041 | 0.575 | 0.286 | 0.046 |
| Follow-Your-Emoji [43] | 20.24 | 0.867 | 0.203 | 0.048 | 0.302 | 0.350 | 0.166 | 0.345 | 0.360 | 0.097 |
| X-Portrait [76] | 19.75 | 0.845 | 0.200 | 0.051 | 0.229 | 0.351 | 0.274 | 0.341 | 0.376 | 0.191 |
| Ours | 26.78 | 0.905 | 0.119 | 0.020 | 0.702 | 0.164 | 0.018 | 0.624 | 0.257 | 0.030 |

Table 3. Quantitative results on the NeRSemble [33] testset.

degrading the final generation quality, we introduce two learnable tokens to differentiate real and synthetic images. To be specific, during data loading, each image is assigned a label based on its origin: “synthetic” for synthetic images and “real” for images sourced from real videos. Each label corresponds to an optimizable vector, which is fed into the cross-attention module during the denoising process. Notably, only the “real” label is used during inference. This strategy enables the model to effectively leverage the diversity of synthetic data while preserving the photorealism of real images.

3.4.3. Discussion

As shown in Table 1, our synthetic dataset contains a significantly larger number of subjects compared to existing multi-view datasets. Moreover, current datasets are captured under strictly controlled lighting conditions, making them unsuitable for training a generalizable head model. In contrast, SphereHead is trained on in-the-wild images, allowing it to reliably simulate diverse lighting conditions. Additionally, having full control over the viewpoints allows us to sample dense head poses, which is crucial for training data-hungry models like diffusion.

4. Experiments

4.1. Implementation Details

We use VFHQ [75], NeRSemble [33], MEAD [66], and our synthetic dataset to train our model. We adopt a two-stage training strategy to learn appearance modeling and temporal consistency separately. In the first stage, we set

the sequence length to 1 and disable all temporal modules. We train the Gaussian attributes along with all remaining parameters in the dual branch. In the second stage, we increase the sequence length to 14. We train the temporal modules while keeping all other parameters fixed. The synthetic dataset is not used in this stage since multi-view frames are not continuous. All the frames are cropped and resized to 512×512 resolution.

For the evaluation, we use two datasets to validate our methods, One is the VFHQ testset [75], which includes 50 talking videos. To further evaluate the motion accuracy in challenging cases, we use the last 20 subjects of NeRSemble [33] as another testset. For each subject we randomly select 2 sequences. Videos of these 20 subjects are excluded from the training dataset.

4.2. Comparisons

We compare our method with ROME [32], Portrait4D-v2 [14], VODOO 3D [63], GAGAvatar [9], Follow-Your-Emoji (F-Y-E) [43], X-Portrait [76]. ROME is a mesh based one-shot avatar. Portrait4D-v2 and VODOO 3D are NeRF based head avatars. GAGAvatar is a 3D Gaussian based head model. Follow-Your-Emoji and X-Portrait are based on video diffusion. We use the first frame as reference image for each sequence on VFHQ. For the NeRSemble testset, we randomly select one frame from the other video sequence of the same subject as the reference. Qualitative comparisons are shown in Figure 4. Our method could generate more expressive and consistent results compared with previous works. We found that when there is a significant difference in poses between the reference and the

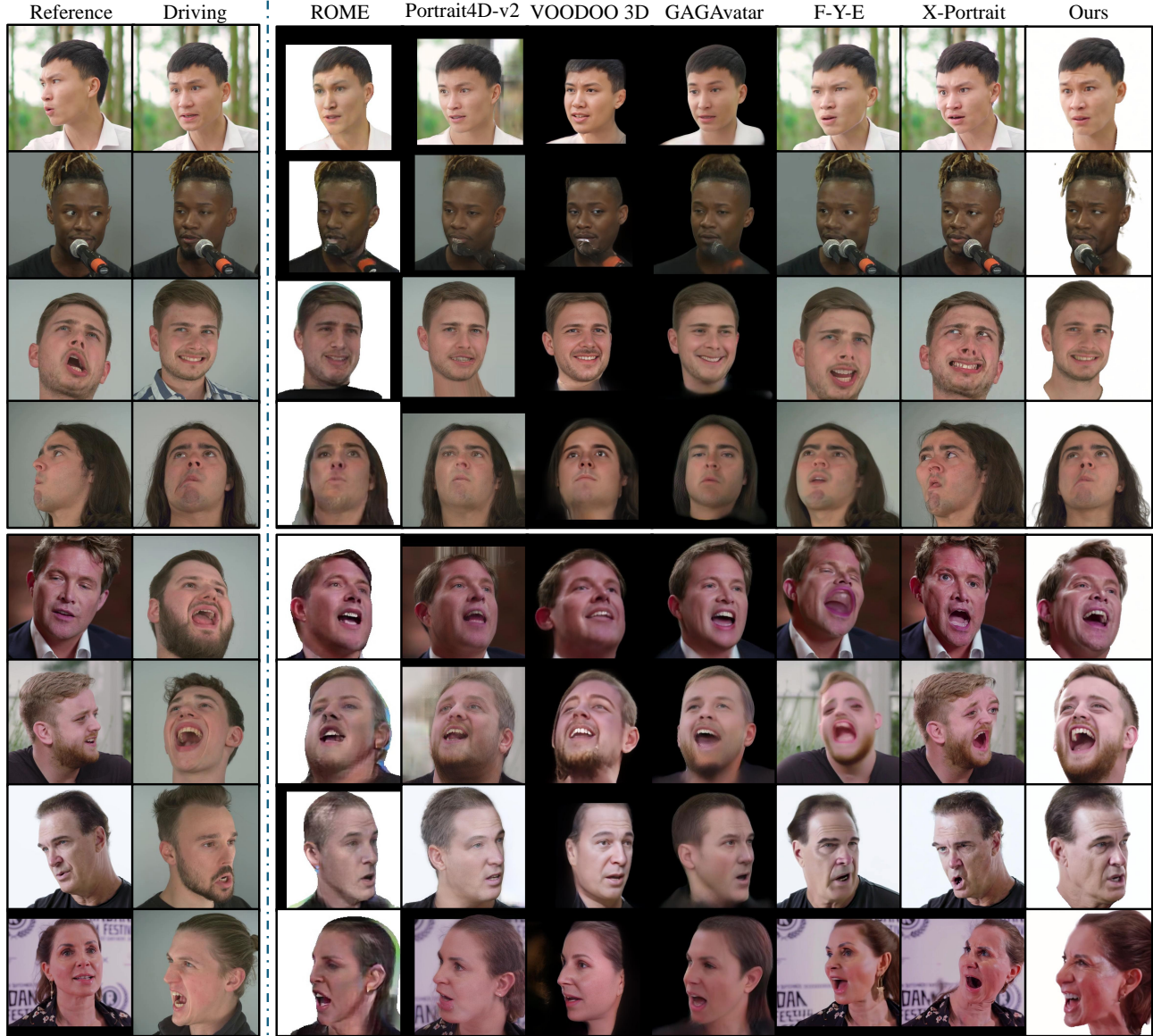


Figure 4. Comparison on the face reenactment task. We found that previous methods often struggled to preserve identity or expressions. In contrast, our approach not only faithfully reconstructs the identity from the reference but also maintains expression accuracy.

driving frame, most methods struggle to effectively preserve the identity information from the reference. ROME often failed to model hair region and facial details because of the limited representation ability of mesh model. We found that Portrait4D-v2, VOODOO 3D, and GAGAvatar often struggled to generate exaggerated expressions and maintain identity when dealing with significant pose deviations. This highlights the limited capacity of traditional one-to-one mapping head models. Follow-Your-Emoji and X-Portrait are trained with publicly available talking head datasets and several hundred internal video sequences. We observed that the results from both methods often exhibit severe facial distortions and inconsistencies. This further

implies the data hungry nature of diffusion models and highlights the necessity of using our synthetic multi-view head dataset. Compared with these methods, our results exhibit much better consistency and motion accuracy, thanks to our learnable control signal representation and synthetic data utilization.

The quantitative results are shown in Table 2 and Table 3. For the self-reenactment task, we evaluate standard metrics such as PSNR, SSIM, LPIPS [93], and L1 distance. We measure identity preservation by comparing the cosine similarity between the embeddings of a face recognition network [12] (CSIM). We compute Average Expression Distance (AED) and Average Pose Distance (APD) to

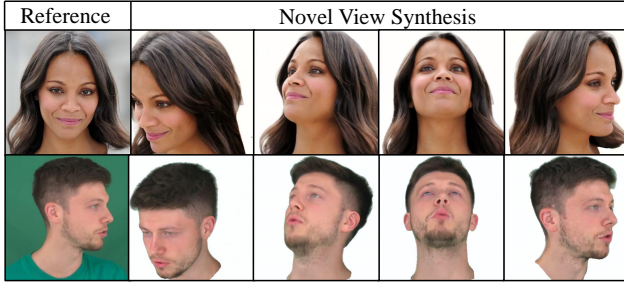


Figure 5. Novel view synthesis results. Given a single reference image, we can freely control the camera to synthesize view-consistent head images.

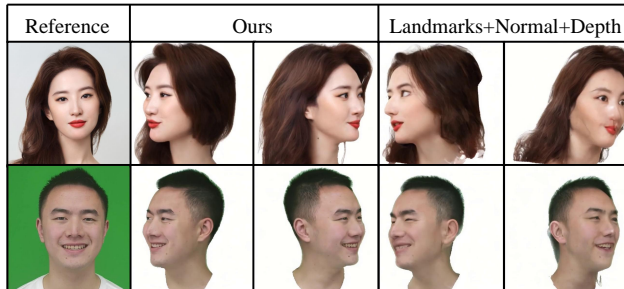


Figure 6. The figure illustrates the head of the reference image at a yaw angle of $\pm 50^\circ$ generated by our model and the baseline diffusion model (controlled by traditional visual cues).

evaluate the head motion accuracy. For fair comparison, we only compute these metrics in the head region. Our method outperforms previous works in all metrics, which further verifies the effectiveness and superiority of our model.

4.3. Novel View Synthesis

To further evaluate the 3D consistency of our model, we conduct a novel view synthesis experiment. Given a single reference image, we manipulate the poses of the generated head images by adjusting the pose parameters of the FLAME head model. As illustrated in Figure 5, our method produces reasonable and consistent results even for large pose variations. This demonstrates that our learnable Gaussian embedding, combined with training on a synthetic dataset, effectively enhances the 3D consistency of diffusion models.

5. Ablation Study

5.1. Learnable Gaussian Embedding

Some previous diffusion based portrait generation models employ landmarks, normal maps, or depth maps as signals to control diffusion generation. To demonstrate the deficiencies of these visual cues, we design a baseline model that concatenate FLAME’s landmarks, normal maps, depth

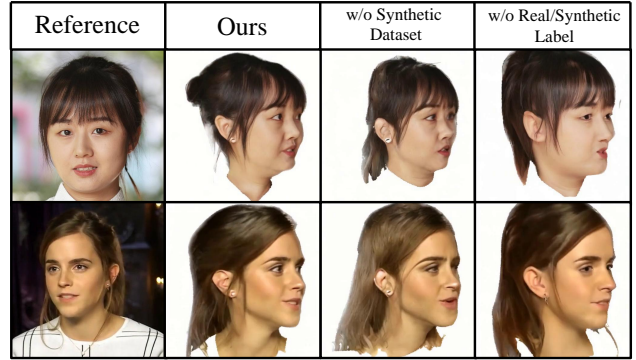


Figure 7. Without training on our synthetic dataset, the model may fail to synthesize head images in large poses. And if the model is trained without Real/Synthetic labels, the artifacts of the synthesized samples may influence the generated results.

maps as control signals. As shown in Figure 6, such a model fails to accurately generate images that meet the required expressions and poses. This primarily stems from the sparsity of landmarks, as well as the low-frequency nature and 3D inconsistency of normal and depth information. Our learnable Gaussian feature map \mathbf{F} is a dense, adaptive, expressive, and 3D consistent control signal representation. It showcased better quality in controlling head motion generation.

5.2. Synthetic Dataset

We utilize a synthetic dataset to enhance the model’s identity generalization and view robustness. Additionally, we incorporate real/synthetic labels to mitigate the impact of artifacts in synthetic data on the generated results. As illustrated in Figure 7, models trained solely on public real datasets struggle to synthesize head images with large poses. Moreover, without our real/synthetic label as input, noticeable artifacts may appear in the generated results.

6. Conclusion and Discussion

In this paper, we enhanced the generalization and 3D consistency of head diffusion through two key innovations: control signal representation and dataset design. First, we introduced splatting-based feature maps derived from learnable Gaussian embeddings, which serve as dense, adaptive, and 3D-consistent control signals. Second, we incorporated synthetic data to improve consistency and generalization, paired with a real/synthetic labeling strategy to mitigate artifacts. Experiments demonstrated that these contributions collectively advance the fidelity and robustness of head generation.

Notably, the framework of augmenting diffusion models with learnable Gaussian embeddings is not restricted to head avatars. We envision extensions to human body animation or generalizable video generation, where 3D-aware

control signals could similarly address consistency challenges. We leave these promising directions for future work.

Acknowledgements. This research was supported by the National Natural Science Foundation of China (No.62441224, No.62272433). The numerical calculations in this paper have been done on the supercomputing system in the Supercomputing Center of University of Science and Technology of China.

References

- [1] Volker Blanz and Thomas Vetter. A morphable model for the synthesis of 3d faces. In *Proceedings of the 26th Annual Conference on Computer Graphics and Interactive Techniques (SIGGRAPH)*, pages 187–194, 1999. 1, 3
- [2] Tim Brooks, Aleksander Holynski, and Alexei A Efros. Instructpix2pix: Learning to follow image editing instructions. In *Proceedings of the IEEE/CVF Conference on Computer Vision and Pattern Recognition*, pages 18392–18402, 2023. 3
- [3] Marcel C Buehler, Gengyan Li, Erroll Wood, Leonhard Helminger, Xu Chen, Tanmay Shah, Daoye Wang, Stephan Garbin, Sergio Orts-Escolano, Otmar Hilliges, et al. Cafca: High-quality novel view synthesis of expressive faces from casual few-shot captures. In *SIGGRAPH Asia 2024 Conference Papers*, pages 1–12, 2024. 2
- [4] Egor Burkov, Igor Pasechnik, Artur Grigorev, and Victor Lempitsky. Neural head reenactment with latent pose descriptors. In *IEEE/CVF Conference on Computer Vision and Pattern Recognition (CVPR)*, 2020. 2
- [5] Chen Cao, Yanlin Weng, Shun Zhou, Yiyong Tong, and Kun Zhou. Facewarehouse: A 3d facial expression database for visual computing. *IEEE Transactions on Visualization and Computer Graphics*, 20(3):413–425, 2013. 1
- [6] Chen Cao, Tomas Simon, Jin Kyu Kim, Gabe Schwartz, Michael Zollhoefer, Shun-Suke Saito, Stephen Lombardi, Shih-En Wei, Danielle Belko, Shoou-I Yu, et al. Authentic volumetric avatars from a phone scan. *ACM Transactions on Graphics (TOG)*, 41(4):1–19, 2022. 2
- [7] Di Chang, Yichun Shi, Quankai Gao, Hongyi Xu, Jessica Fu, Guoxian Song, Qing Yan, Yizhe Zhu, Xiao Yang, and Mohammad Soleymani. Magicpose: Realistic human poses and facial expressions retargeting with identity-aware diffusion. In *Forty-first International Conference on Machine Learning, ICML 2024, Vienna, Austria, July 21-27, 2024*. OpenReview.net, 2024. 5
- [8] Xiyi Chen, Marko Mihajlovic, Shaofei Wang, Sergey Prokudin, and Siyu Tang. Morphable diffusion: 3d-consistent diffusion for single-image avatar creation. In *Proceedings of the IEEE/CVF Conference on Computer Vision and Pattern Recognition*, pages 10359–10370, 2024. 3
- [9] Xuangeng Chu and Tatsuya Harada. Generalizable and animatable gaussian head avatar. In *The Thirty-eighth Annual Conference on Neural Information Processing Systems*, 2024. 1, 2, 6
- [10] Xuangeng Chu, Yu Li, Ailing Zeng, Tianyu Yang, Lijian Lin, Yunfei Liu, and Tatsuya Harada. GPAvatar: Generalizable and precise head avatar from image(s). In *The Twelfth International Conference on Learning Representations*, 2024. 2
- [11] Darren Cosker, Eva Krumbhuber, and Adrian Hilton. A facs valid 3d dynamic action unit database with applications to 3d dynamic morphable facial modeling. In *2011 international conference on computer vision*, pages 2296–2303. IEEE, 2011. 5
- [12] Jiankang Deng, Jia Guo, Niannan Xue, and Stefanos Zafeiriou. Arcface: Additive angular margin loss for deep face recognition. In *Proceedings of the IEEE/CVF conference on computer vision and pattern recognition*, pages 4690–4699, 2019. 7, 1
- [13] Yu Deng, Duomin Wang, Xiaohang Ren, Xingyu Chen, and Baoyuan Wang. Portrait4d: Learning one-shot 4d head avatar synthesis using synthetic data. In *Proceedings of the IEEE/CVF Conference on Computer Vision and Pattern Recognition*, pages 7119–7130, 2024. 1, 2
- [14] Yu Deng, Duomin Wang, and baoyuan Wang. Portrait4d-v2: Pseudo multi-view data creates better 4d head synthesizer. In *ECCV*, 2024. 1, 2, 6
- [15] Nikita Drobyshev, Jenya Chelishev, Taras Khakhulin, Aleksei Ivakhnenko, Victor Lempitsky, and Egor Zakharov. Megaportraits: One-shot megapixel neural head avatars. In *Proceedings of the 30th ACM International Conference on Multimedia*, pages 2663–2671, 2022. 2
- [16] Nikita Drobyshev, Antoni Bigata Casademunt, Konstantinos Vougioukas, Zoe Landgraf, Stavros Petridis, and Maja Pantic. Emoportraits: Emotion-enhanced multimodal one-shot head avatars. In *Proceedings of the IEEE Conference on Computer Vision and Pattern Recognition (CVPR)*, 2024. 2
- [17] Dimitrios Gerogiannis, Foivos Paraperas Papanтониου, Rolandos Alexandros Potamias, Alexandros Lattas, and Stefanos Zafeiriou. Arc2avatar: Generating expressive 3d avatars from a single image via id guidance. *arXiv preprint arXiv:2501.05379*, 2025. 3
- [18] Partha Ghosh, Pravir Singh Gupta, Roy Uziel, Anurag Ranjan, Michael Black, and Timo Bolkart. Gif: Generative interpretable faces. In *3DV*, 2020. 3
- [19] Simon Giebenhain, Tobias Kirschstein, Markos Georgopoulos, Martin Rünz, Lourdes Agapito, and Matthias Nießner. Learning neural parametric head models. In *Proc. IEEE Conf. on Computer Vision and Pattern Recognition (CVPR)*, 2023. 2
- [20] Yuming Gu, Hongyi Xu, You Xie, Guoxian Song, Yichun Shi, Di Chang, Jing Yang, and Linjie Luo. Diffportrait3d: Controllable diffusion for zero-shot portrait view synthesis. In *Proceedings of the IEEE/CVF Conference on Computer Vision and Pattern Recognition (CVPR)*, pages 10456–10465, 2024. 3
- [21] Jiazhi Guan, Quanwei Yang, Kaisiyuan Wang, Hang Zhou, Shengyi He, Zhiliang Xu, Haocheng Feng, Errui Ding, Jingdong Wang, Hongtao Xie, et al. Talk-act: Enhance textural-awareness for 2d speaking avatar reenactment with

- diffusion model. In *SIGGRAPH Asia 2024 Conference Papers*, pages 1–11, 2024. 3
- [22] Jianzhu Guo, Dingyun Zhang, Xiaoqiang Liu, Zhizhou Zhong, Yuan Zhang, Pengfei Wan, and Di Zhang. Live-portrait: Efficient portrait animation with stitching and re-targeting control. *arXiv preprint arXiv:2407.03168*, 2024. 2
- [23] Yue Han, Junwei Zhu, Keke He, Xu Chen, Yanhao Ge, Wei Li, Xiangtai Li, Jiangning Zhang, Chengjie Wang, and Yong Liu. Face-adapter for pre-trained diffusion models with fine-grained id and attribute control. In *European Conference on Computer Vision*, pages 20–36. Springer, 2024. 3
- [24] Xu He, Xiaoyu Li, Di Kang, Jiangnan Ye, Chaopeng Zhang, Liyang Chen, Xiangjun Gao, Han Zhang, Zhiyong Wu, and Haolin Zhuang. Magicman: Generative novel view synthesis of humans with 3d-aware diffusion and iterative refinement. *arXiv preprint arXiv:2408.14211*, 2024. 3
- [25] Jonathan Ho, Ajay Jain, and Pieter Abbeel. Denoising diffusion probabilistic models. In *Advances in Neural Information Processing Systems 33: Annual Conference on Neural Information Processing Systems 2020, NeurIPS 2020, December 6-12, 2020, virtual*, 2020. 3
- [26] Fa-Ting Hong and Dan Xu. Implicit identity representation conditioned memory compensation network for talking head video generation. In *ICCV*, 2023. 2
- [27] Fa-Ting Hong, Longhao Zhang, Li Shen, and Dan Xu. Depth-aware generative adversarial network for talking head video generation. In *Proceedings of the IEEE/CVF conference on computer vision and pattern recognition*, pages 3397–3406, 2022. 2
- [28] Yang Hong, Bo Peng, Haiyao Xiao, Ligang Liu, and Juyong Zhang. Headnerf: A real-time nerf-based parametric head model. In *IEEE/CVF Conference on Computer Vision and Pattern Recognition (CVPR)*, 2022. 1, 2
- [29] Li Hu. Animate anyone: Consistent and controllable image-to-video synthesis for character animation. In *Proceedings of the IEEE/CVF Conference on Computer Vision and Pattern Recognition*, pages 8153–8163, 2024. 5
- [30] Yash Kant, Ethan Weber, Jin Kyu Kim, Rawal Khirodkar, Su Zhaoen, Julieta Martinez, Igor Gilitschenski, Shunsuke Saito, and Timur Bagautdinov. Pippo: High-resolution multi-view humans from a single image. *arXiv preprint arXiv:2502.07785*, 2025. 3
- [31] Bernhard Kerbl, Georgios Kopanas, Thomas Leimkühler, and George Drettakis. 3d gaussian splatting for real-time radiance field rendering. *ACM Transactions on Graphics*, 42(4), 2023. 2, 4
- [32] Taras Khakhulin, Vanessa Sklyarova, Victor Lempitsky, and Egor Zakharov. Realistic one-shot mesh-based head avatars. In *European Conference of Computer vision (ECCV)*, 2022. 2, 6
- [33] Tobias Kirschstein, Shenhan Qian, Simon Giebenhain, Tim Walter, and Matthias Nießner. Nersemble: Multi-view radiance field reconstruction of human heads. *ACM Trans. Graph.*, 42(4), 2023. 5, 6, 1
- [34] Tobias Kirschstein, Simon Giebenhain, and Matthias Nießner. Diffusionavatars: Deferred diffusion for high-fidelity 3d head avatars. In *Proceedings of the IEEE/CVF Conference on Computer Vision and Pattern Recognition*, pages 5481–5492, 2024. 3
- [35] Yushi Lan, Feitong Tan, Di Qiu, Qiangeng Xu, Kyle Genova, Zeng Huang, Sean Fanello, Rohit Pandey, Thomas Funkhouser, Chen Change Loy, and Yinda Zhang. Gaussian3diff: 3d gaussian diffusion for 3d full head synthesis and editing. In *ECCV*, 2024. 3
- [36] Heyuan Li, Ce Chen, Tianhao Shi, Yuda Qiu, Sizhe An, Guanying Chen, and Xiaoguang Han. Spherehead: stable 3d full-head synthesis with spherical tri-plane representation. In *European Conference on Computer Vision*, pages 324–341. Springer, 2024. 2, 5
- [37] Tianye Li, Timo Bolkart, Michael J. Black, Hao Li, and Javier Romero. Learning a model of facial shape and expression from 4D scans. *ACM Transactions on Graphics, (Proc. SIGGRAPH Asia)*, 36(6):194:1–194:17, 2017. 2, 4, 5
- [38] Tianye Li, Timo Bolkart, Michael J Black, Hao Li, and Javier Romero. Learning a model of facial shape and expression from 4d scans. *ACM Trans. Graph.*, 36(6):194–1, 2017. 1
- [39] Weichuang Li, Longhao Zhang, Dong Wang, Bin Zhao, Zhigang Wang, Mulin Chen, Bang Zhang, Zhongjian Wang, Liefeng Bo, and Xuelong Li. One-shot high-fidelity talking-head synthesis with deformable neural radiance field. In *Proceedings of the IEEE/CVF Conference on Computer Vision and Pattern Recognition*, pages 17969–17978, 2023. 2
- [40] Xueting Li, Shalini De Mello, Sifei Liu, Koki Nagano, Umar Iqbal, and Jan Kautz. Generalizable one-shot neural head avatar. *NeurIPS*, 2023. 1
- [41] Xueting Li, Shalini De Mello, Sifei Liu, Koki Nagano, Umar Iqbal, and Jan Kautz. Generalizable one-shot 3d neural head avatar. *Advances in Neural Information Processing Systems*, 36, 2024. 2
- [42] Yixing Lu, Junting Dong, Youngjoong Kwon, Qin Zhao, Bo Dai, and Fernando De la Torre. Gas: Generative avatar synthesis from a single image. *arXiv preprint arXiv:2502.06957*, 2025. 3
- [43] Yue Ma, Hongyu Liu, Hongfa Wang, Heng Pan, Yingqing He, Junkun Yuan, Ailing Zeng, Chengfei Cai, Heung-Yeung Shum, Wei Liu, et al. Follow-your-emoji: Fine-controllable and expressive freestyle portrait animation. In *ACM SIGGRAPH Asia Conference Proceedings*, 2024. 3, 6
- [44] Zhiyuan Ma, Xiangyu Zhu, Guo-Jun Qi, Zhen Lei, and Lei Zhang. Otavatar: One-shot talking face avatar with controllable tri-plane rendering. In *Proceedings of the IEEE/CVF Conference on Computer Vision and Pattern Recognition*, pages 16901–16910, 2023. 2
- [45] Arun Mallya, Ting-Chun Wang, and Ming-Yu Liu. Implicit warping for animation with image sets. In *Conference on Neural Information Processing Systems (NeurIPS)*, 2022. 2
- [46] Mohit Mendiratta, Xingang Pan, Mohamed Elgharib, Kartik Teotia, Mallikarjun B R, Ayush Tewari, Vladislav

- Golyanik, Adam Kortylewski, and Christian Theobalt. Avatarstudio: Text-driven editing of 3d dynamic human head avatars, 2023. 3
- [47] Ben Mildenhall, Pratul P. Srinivasan, Matthew Tancik, Jonathan T. Barron, Ravi Ramamoorthi, and Ren Ng. Nerf: Representing scenes as neural radiance fields for view synthesis. In *ECCV*, 2020. 2
- [48] Mirela Ostrek and Justus Thies. Stable video portraits. In *European Conference on Computer Vision (ECCV 2024)*. Springer Cham, 2024. 3
- [49] Dongwei Pan, Long Zhuo, Jingtian Piao, Huiwen Luo, Wei Cheng, Yuxin Wang, Siming Fan, Shengqi Liu, Lei Yang, Bo Dai, Ziwei Liu, Chen Change Loy, Chen Qian, Wayne Wu, Dahua Lin, and Kwan-Yee Lin. Renderme-360: Large digital asset library and benchmark towards high-fidelity head avatars. In *Thirty-seventh Conference on Neural Information Processing Systems Datasets and Benchmarks Track*, 2023. 5
- [50] Foivos Paraperas Papantoniou, Alexandros Lattas, Stylianos Moschoglou, Jiankang Deng, Bernhard Kainz, and Stefanos Zafeiriou. Arc2face: A foundation model for id-consistent human faces. In *Proceedings of the European Conference on Computer Vision (ECCV)*, 2024. 3
- [51] Malte Prinzler, Egor Zakharov, Vanessa Sklyarova, Berna Kabadayi, and Justus Thies. Joker: Conditional 3d head synthesis with extreme facial expressions. In *3DV*, 2025. 3
- [52] Yurui Ren, Ge Li, Yuanqi Chen, Thomas H. Li, and Shan Liu. Pirenderer: Controllable portrait image generation via semantic neural rendering. In *Proceedings of the IEEE/CVF International Conference on Computer Vision (ICCV)*, 2021. 3
- [53] George Retsinas, Panagiotis P Filntisis, Radek Danecek, Victoria F Abrevaya, Anastasios Roussos, Timo Bolkart, and Petros Maragos. 3d facial expressions through analysis-by-neural-synthesis. In *Proceedings of the IEEE/CVF Conference on Computer Vision and Pattern Recognition*, pages 2490–2501, 2024. 2, 1
- [54] Robin Rombach, Andreas Blattmann, Dominik Lorenz, Patrick Esser, and Björn Ommer. High-resolution image synthesis with latent diffusion models. In *Proceedings of the IEEE/CVF conference on computer vision and pattern recognition*, pages 10684–10695, 2022. 3, 4
- [55] Tim Salimans and Jonathan Ho. Progressive distillation for fast sampling of diffusion models. In *International Conference on Learning Representations*, 2022. 5
- [56] Aliaksandr Siarohin, Stéphane Lathuilière, Sergey Tulyakov, Elisa Ricci, and Nicu Sebe. First order motion model for image animation. In *Conference on Neural Information Processing Systems (NeurIPS)*, 2019. 2
- [57] Aliaksandr Siarohin, Oliver Woodford, Jian Ren, Menglei Chai, and Sergey Tulyakov. Motion representations for articulated animation. In *CVPR*, 2021. 2
- [58] Jingxiang Sun, Xuan Wang, Lizhen Wang, Xiaoyu Li, Yong Zhang, Hongwen Zhang, and Yebin Liu. Next3d: Generative neural texture rasterization for 3d-aware head avatars. In *Proceedings of the IEEE/CVF Conference on Computer Vision and Pattern Recognition*, pages 20991–21002, 2023. 1, 2
- [59] Jiapeng Tang, Davide Davoli, Tobias Kirschstein, Liam Schoneveld, and Matthias Niessner. Gaf: Gaussian avatar reconstruction from monocular videos via multi-view diffusion. *arXiv preprint arXiv:2412.10209*, 2024. 3
- [60] Ayush Tewari, Mohamed Elgharib, Gaurav Bharaj, Florian Bernard, Hans-Peter Seidel, Patrick Pérez, Michael Zollhöfer, and Christian Theobalt. Stylerig: Rigging stylegan for 3d control over portrait images. In *Proceedings of the IEEE Conference on Computer Vision and Pattern Recognition (CVPR)*, 2020. 3
- [61] Luan Tran and Xiaoming Liu. Nonlinear 3d face morphable model. In *Proceedings of the IEEE conference on computer vision and pattern recognition*, pages 7346–7355, 2018. 1
- [62] Phong Tran, Egor Zakharov, Long-Nhat Ho, Liwen Hu, Adilbek Karmanov, Aviral Agarwal, McLean Goldwhite, Ariana Bermudez Venegas, Anh Tuan Tran, and Hao Li. Voodoo xp: Expressive one-shot head reenactment for vr telepresence. *arXiv preprint arXiv:2405.16204*, 2024. 1, 2
- [63] Phong Tran, Egor Zakharov, Long-Nhat Ho, Anh Tuan Tran, Liwen Hu, and Hao Li. Voodoo 3d: Volumetric portrait disentanglement for one-shot 3d head reenactment. In *Proceedings of the IEEE/CVF Conference on Computer Vision and Pattern Recognition*, pages 10336–10348, 2024. 1, 2, 6
- [64] Ashish Vaswani, Noam Shazeer, Niki Parmar, Jakob Uszkoreit, Llion Jones, Aidan N Gomez, Łukasz Kaiser, and Illia Polosukhin. Attention is all you need. In *Advances in Neural Information Processing Systems*. Curran Associates, Inc., 2017. 4
- [65] Duomin Wang, Yu Deng, Zixin Yin, Heung-Yeung Shum, and Baoyuan Wang. Progressive disentangled representation learning for fine-grained controllable talking head synthesis. In *Proceedings of the IEEE Conference on Computer Vision and Pattern Recognition (CVPR)*, 2023. 2
- [66] Kaisiyuan Wang, Qianyi Wu, Linsen Song, Zhuoqian Yang, Wayne Wu, Chen Qian, Ran He, Yu Qiao, and Chen Change Loy. Mead: A large-scale audio-visual dataset for emotional talking-face generation. In *European conference on computer vision*, pages 700–717. Springer, 2020. 5, 6, 1
- [67] Qixun Wang, Xu Bai, Haofan Wang, Zekui Qin, and Anthony Chen. Instantid: Zero-shot identity-preserving generation in seconds. *arXiv preprint arXiv:2401.07519*, 2024. 3
- [68] Tengfei Wang, Bo Zhang, Ting Zhang, Shuyang Gu, Jianmin Bao, Tadas Baltrusaitis, Jingjing Shen, Dong Chen, Fang Wen, Qifeng Chen, et al. Rodin: A generative model for sculpting 3d digital avatars using diffusion. In *Proceedings of the IEEE/CVF Conference on Computer Vision and Pattern Recognition*, pages 4563–4573, 2023. 2, 3
- [69] Ting-Chun Wang, Arun Mallya, and Ming-Yu Liu. One-shot free-view neural talking-head synthesis for video conferencing. In *Proceedings of the IEEE Conference on Computer Vision and Pattern Recognition*, 2021. 2
- [70] Huawei Wei, Zejun Yang, and Zhisheng Wang. Anipor-trait: Audio-driven synthesis of photorealistic portrait animations, 2024. 3
- [71] Yue Wu, Yu Deng, Jiaolong Yang, Fangyun Wei, Chen Qifeng, and Xin Tong. Anifacegan: Animatable 3d-aware

- face image generation for video avatars. In *Advances in Neural Information Processing Systems*, 2022. 2
- [72] Yue Wu, Sicheng Xu, Jianfeng Xiang, Fangyun Wei, Qifeng Chen, Jiaolong Yang, and Xin Tong. Aniportrait-gan: Animatable 3d portrait generation from 2d image collections. In *SIGGRAPH Asia 2023 Conference Proceedings*, 2023. 2
- [73] Cheng-hsin Wu, Ningyuan Zheng, Scott Ardisson, Rohan Bali, Danielle Belko, Eric Brockmeyer, Lucas Evans, Timothy Godisart, Hyowon Ha, Xuhua Huang, Alexander Hypes, Taylor Koska, Steven Krenn, Stephen Lombardi, Xiaomin Luo, Kevyn McPhail, Laura Millerschoen, Michal Perdoch, Mark Pitts, Alexander Richard, Jason Saragih, Junko Saragih, Takaaki Shiratori, Tomas Simon, Matt Stewart, Autumn Trimble, Xinshuo Weng, David Whitewolf, Chenglei Wu, Shou-I Yu, and Yaser Sheikh. Multiface: A dataset for neural face rendering. In *arXiv*, 2022. 5
- [74] Jun Xiang, Xuan Gao, Yudong Guo, and Juyong Zhang. Flashavatar: High-fidelity head avatar with efficient gaussian embedding. In *The IEEE Conference on Computer Vision and Pattern Recognition (CVPR)*, 2024. 4
- [75] Liangbin Xie, Xintao Wang, Honglun Zhang, Chao Dong, and Ying Shan. Vfhq: A high-quality dataset and benchmark for video face super-resolution. In *The IEEE Conference on Computer Vision and Pattern Recognition Workshops (CVPRW)*, 2022. 6, 1
- [76] You Xie, Hongyi Xu, Guoxian Song, Chao Wang, Yichun Shi, and Linjie Luo. X-portrait: Expressive portrait animation with hierarchical motion attention. In *ACM SIGGRAPH 2024 Conference Papers, SIGGRAPH 2024, Denver, CO, USA, 27 July 2024- 1 August 2024*, page 115. ACM, 2024. 3, 6
- [77] Sicheng Xu, Jiaolong Yang, Dong Chen, Fang Wen, Yu Deng, Yunde Jia, and Xin Tong. Deep 3d portrait from a single image. In *Proceedings of the IEEE/CVF Conference on Computer Vision and Pattern Recognition*, pages 7710–7720, 2020. 2
- [78] Yuelang Xu, Lizhen Wang, Zerong Zheng, Zhaoqi Su, and Yebin Liu. 3d gaussian parametric head model. In *European Conference on Computer Vision*, pages 129–147. Springer, 2024. 1, 2
- [79] Ziyi Xu, Ziyao Huang, Juan Cao, Yong Zhang, Xiaodong Cun, Qing Shuai, Yuchen Wang, Linchao Bao, Jintao Li, and Fan Tang. Anchorcrafter: Animate cyberanchors saling your products via human-object interacting video generation. *arXiv preprint arXiv:2411.17383*, 2024. 3
- [80] Zhongcong Xu, Jianfeng Zhang, Jun Hao Liew, Han-shu Yan, Jia-Wei Liu, Chenxu Zhang, Jiashi Feng, and Mike Zheng Shou. Magicanimate: Temporally consistent human image animation using diffusion model. In *IEEE/CVF Conference on Computer Vision and Pattern Recognition (CVPR)*, 2024. 5
- [81] Haijie Yang, Zhenyu Zhang, Hao Tang, Jianjun Qian, and Jian Yang. Consistentavatar: Learning to diffuse fully consistent talking head avatar with temporal guidance. In *Proceedings of the 32nd ACM International Conference on Multimedia, MM 2024, Melbourne, VIC, Australia, 28 October 2024 - 1 November 2024*, pages 3964–3973. ACM, 2024. 3
- [82] Quanwei Yang, Jiazhi Guan, Kaisiyuan Wang, Lingyun Yu, Wenqing Chu, Hang Zhou, ZhiQiang Feng, Haocheng Feng, Errui Ding, Jingdong Wang, et al. Showmaker: Creating high-fidelity 2d human video via fine-grained diffusion modeling. *Advances in Neural Information Processing Systems*, 37:51039–51062, 2025. 3
- [83] Shurong Yang, Huadong Li, Juhao Wu, Minhao Jing, Linze Li, Renhe Ji, Jiajun Liang, and Haoqiang Fan. Megactor: Harness the power of raw video for vivid portrait animation, 2024. 3
- [84] Zhenhui Ye, Tianyun Zhong, Yi Ren, Jiaqi Yang, Weichuang Li, Jiawei Huang, Ziyue Jiang, Jinzheng He, Rongjie Huang, Jinglin Liu, Chen Zhang, Xiang Yin, Zejun Ma, and Zhou Zhao. Real3d-portrait: One-shot realistic 3d talking portrait synthesis. In *The Twelfth International Conference on Learning Representations, ICLR 2024, Vienna, Austria, May 7-11, 2024*. OpenReview.net, 2024. 2
- [85] Tarun Yenamandra, Ayush Tewari, Florian Bernard, Hans-Peter Seidel, Mohamed Elgharib, Daniel Cremers, and Christian Theobalt. i3dmm: Deep implicit 3d morphable model of human heads. In *IEEE/CVF Conference on Computer Vision and Pattern Recognition (CVPR)*, pages 12803–12813, 2021. 2, 5
- [86] Fei Yin, Yong Zhang, Xiaodong Cun, Mingdeng Cao, Yanbo Fan, Xuan Wang, Qingyan Bai, Baoyuan Wu, Jue Wang, and Yujiu Yang. Styleheat: One-shot high-resolution editable talking face generation via pre-trained stylegan. In *European Conference of Computer vision (ECCV)*, 2022. 3
- [87] Wangbo Yu, Yanbo Fan, Yong Zhang, Xuan Wang, Fei Yin, Yunpeng Bai, Yan-Pei Cao, Ying Shan, Yang Wu, Zhongqian Sun, et al. Nofa: Nerf-based one-shot facial avatar reconstruction. In *ACM SIGGRAPH 2023 Conference Proceedings*, pages 1–12, 2023. 2
- [88] Zhixuan Yu, Jae Shin Yoon, In Kyu Lee, Prashanth Venkatesh, Jaesik Park, Jihun Yu, and Hyun Soo Park. Humbi: A large multiview dataset of human body expressions. In *Proceedings of the IEEE/CVF Conference on Computer Vision and Pattern Recognition*, pages 2990–3000, 2020. 5
- [89] Egor Zakharov, Aliaksandra Shysheya, Egor Burkov, and Victor Lempitsky. Few-shot adversarial learning of realistic neural talking head models. In *ICCV*, 2019. 2
- [90] Bohan Zeng, Xuhui Liu, Sicheng Gao, Boyu Liu, Hong Li, Jianzhuang Liu, and Baochang Zhang. Face animation with an attribute-guided diffusion model. In *Proceedings of the IEEE/CVF Conference on Computer Vision and Pattern Recognition*, pages 628–637, 2023. 3
- [91] Bowen Zhang, Yiji Cheng, Chunyu Wang, Ting Zhang, Jiaolong Yang, Yansong Tang, Feng Zhao, Dong Chen, and Baining Guo. Rodinhd: High-fidelity 3d avatar generation with diffusion models. In *European Conference on Computer Vision*, pages 465–483. Springer, 2024. 2, 3
- [92] Longwen Zhang, Qiwei Qiu, Hongyang Lin, Qixuan Zhang, Cheng Shi, Wei Yang, Ye Shi, Sibe Yang, Lan Xu,

- and Jingyi Yu. Dreamface: Progressive generation of animatable 3d faces under text guidance. *ACM Trans. Graph.*, 42(4):138:1–138:16, 2023. 3
- [93] Richard Zhang, Phillip Isola, Alexei A Efros, Eli Shechtman, and Oliver Wang. The unreasonable effectiveness of deep features as a perceptual metric. In *CVPR*, 2018. 7, 1
- [94] Wenxuan Zhang, Xiaodong Cun, Xuan Wang, Yong Zhang, Xi Shen, Yu Guo, Ying Shan, and Fei Wang. Sadtalker: Learning realistic 3d motion coefficients for stylized audio-driven single image talking face animation. In *Proceedings of the IEEE Conference on Computer Vision and Pattern Recognition (CVPR)*, 2023. 3
- [95] Jian Zhao and Hui Zhang. Thin-plate spline motion model for image animation. In *Proceedings of the IEEE Conference on Computer Vision and Pattern Recognition*, 2022. 2
- [96] Wenliang Zhao, Yongming Rao, Weikang Shi, Zuyan Liu, Jie Zhou, and Jiwen Lu. Diffswap: High-fidelity and controllable face swapping via 3d-aware masked diffusion. *CVPR*, 2023. 3
- [97] Mingwu Zheng, Hongyu Yang, Di Huang, and Liming Chen. Imface: A nonlinear 3d morphable face model with implicit neural representations. In *Proceedings of the IEEE/CVF Conference on Computer Vision and Pattern Recognition*, pages 20343–20352, 2022. 2
- [98] Hang Zhou, Yasheng Sun, Wayne Wu, Chen Change Loy, Xiaogang Wang, and Ziwei Liu. Pose-controllable talking face generation by implicitly modularized audio-visual representation. In *Proceedings of the IEEE Conference on Computer Vision and Pattern Recognition (CVPR)*, 2021. 2
- [99] Jingkai Zhou, Benzhi Wang, Weihua Chen, Jingqi Bai, Dongyang Li, Aixi Zhang, Hao Xu, Mingyang Yang, and Fan Wang. Realisdance: Equip controllable character animation with realistic hands. *arXiv preprint arXiv:2409.06202*, 2024. 3, 5, 1
- [100] Hao Zhu, Haotian Yang, Longwei Guo, Yidi Zhang, Yanru Wang, Mingkai Huang, Menghua Wu, Qiu Shen, Ruigang Yang, and Xun Cao. Facescape: 3d facial dataset and benchmark for single-view 3d face reconstruction. *IEEE Transactions on Pattern Analysis and Machine Intelligence (TPAMI)*, 2023. 5
- [101] Shenhao Zhu, Junming Leo Chen, Zuo Zhuo Dai, Yinghui Xu, Xun Cao, Yao Yao, Hao Zhu, and Siyu Zhu. Champ: Controllable and consistent human image animation with 3d parametric guidance. In *European Conference on Computer Vision (ECCV)*, 2024. 3
- [102] Yiyu Zhuang, Hao Zhu, Xusen Sun, and Xun Cao. Mofan-erf: Morphable facial neural radiance field. In *European Conference on Computer Vision*, pages 268–285. Springer, 2022. 1, 2

Controlling Avatar Diffusion with Learnable Gaussian Embedding

Supplementary Material

A. Dataset Details

We use VFHQ [75], NeRSemble [33], MEAD [66], and our synthetic dataset to train our model.

VFHQ VFHQ is a talking video dataset containing approximately 16,000 subjects. While most videos in this dataset are of high quality, the head movement within each sequence is relatively limited.

NeRSemble NeRSemble consists of 16 viewpoints and 268 subjects. It recorded many exaggerated expressions. We randomly sampled about 4000 sequences from this dataset for training. The last 20 subjects are excluded from training dataset and left for evaluation.

MEAD MEAD consists of 7 viewpoints and 48 subjects. We randomly sampled about 2000 sequences from this dataset for training.

B. Implementation Details

We use a model similar to [53] to track the video datasets. For the synthetic multi-view dataset, we get the FLAME parameters and camera parameters through multi-view landmarks fitting. The dataset sampling probabilities (VFHQ, NeRSemble, MEAD, synthetic) are set to 1:0.8:0.2:1 for the first stage and 1:0.8:0.2:0 for the second stage. The UV resolution of the Gaussians is 256×256 . The latent channels of \mathbf{F} is 8. We use the pose guidance network in [99] to encode our learnable control signals \mathbf{F} into U-Net. The pose guidance network accepts the signals as single modal with channels 8. \tanh is used to make the features in $[-1, 1]$.

C. Evaluation Details

C.1. Metrics

LPIPS. We use the VGG based perceptual similarity metric LPIPS [93] to measure the perceptual similarity between the animated and the driving images.

AED. AED is the mean \mathcal{L}_1 distance of the expression parameters between the animated and the driving images. These parameters, which include facial movement, eyelid, and jaw pose parameters, are extracted by the state-of-the-art 3D face reconstruction method SMIRK [53].

APD. APD is the mean \mathcal{L}_1 distance of the pose parameters between the animated and the driving images. The pose parameters are extracted by SMIRK [53].

CSIM. CSIM measures the identity preservation between two images, through the cosine similarity of two embeddings from a pretrained face recognition network [12]. For self-reenactment, the CSIM is calculated between the animated and the driving images. For cross-reenactment, the CSIM is calculated between the animated and the source portraits.

D. More Results on Cross-identity Reenactment

We show more cross-identity reenactment results in Figure 8

E. Limitations

Although our works have showcased remarkable improvements compared with previous works, it still have some limitations. Our method still relies on a head tracking algorithm to get the control signals. Therefore, large errors in tracking, especially global pose errors, may cause misalignment. The bias of the datasets may also influence the generated results.

F. Broader Impact

Given a single reference image, our model generate consistent and expressive head animation in arbitrary expressions and poses. However, there is a risk of misuse, *e.g.* the so-called DeepFakes. We strongly discourage using our work to generate fake images or videos of individuals with the intent of spreading false information or damaging their reputations. Unfortunately, we may be unable to prevent the nefarious use of our technology. Nevertheless, we believe that performing research in an open and transparent way could raise the public’s awareness of nefarious uses, and our work could further enhance forgery detection capabilities.

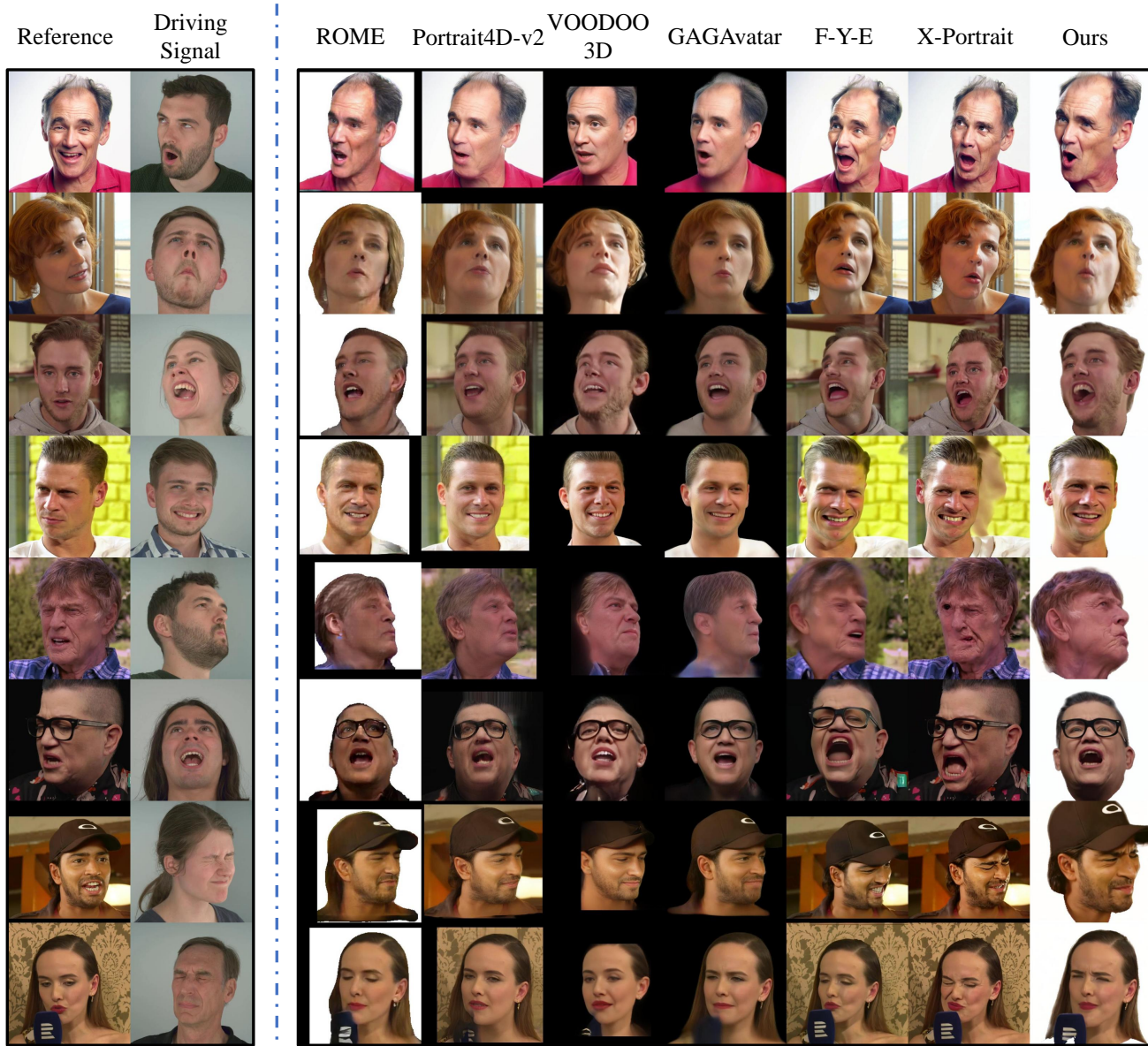


Figure 8. More results on cross-identity reenactment